Sulfur Isotopic Fractionation in the Gas-Phase Oxidation of Sulfur Dioxide Initiated by Hydroxyl Radicals

Fok-Yan Leung, A. J. Colussi,* and M. R. Hoffmann*

W. M. Keck Laboratories, California Institute of Technology, Pasadena, California 91125

Received: March 19, 2001; In Final Form: June 11, 2001

The sulfur isotopic signature of atmospheric sulfate aerosol reflects not only the chemical and isotopic composition of its precursors, but also their oxidation pathways. Thus, to trace back the sources of sulfate, a quantitative assessment of sulfur isotopes fractionation in major atmospheric processes is required. In this paper, we evaluate S-isotope fractionation ratios $f = (k_{OH+^{34}SO_2})/(k_{OH+^{32}SO_2})$ for the gas-phase oxidation of SO_2 by OH-radicals, using RRKM transition-state theory. Calculations were constrained by reliable rates for the $HO + {}^{32}SO_2 + M = HO^{32}SO_2 + M$ reaction, an ab initio transition-state structure, and actual spectroscopic data for the sulfur isotopomers of the hydroxysulfonyl $HOSO_2$ radical. By assuming plausible Lennard-Jones parameters for $HOSO_2$ collisions with N_2 as bath gas, which are consistent with the experimental values of $\langle \Delta E_{down} \rangle \sim 200$ cm^{-1} and a collisional efficiency of $\beta_c \sim 0.2$ in air, we derive $f > 1$ values at the temperatures and pressures prevalent in the terrestrial atmosphere below 30 km. Present results rationalize the evolution of stratospheric aerosol sulfur isotopic composition after volcanic SO_2 injections above 15 km and the ^{34}S enrichment of tropospheric sulfate aerosol during the summer months.

Introduction

Sulfur compounds play an important role in atmospheric chemistry. Some species, such as sulfur dioxide, present at pptv−ppbv levels over remote and urban areas, respectively,[1] are largely anthropogenic, but others, such as dimethyl sulfide and carbon disulfide, are produced by bacterial reduction of marine sulfate.[2] The relatively fast oxidation of sulfur dioxide in the boundary layer is relevant to air pollution and acid rain.[3] In contrast, the slow oxidation of carbonyl sulfide, the most abundant sulfur species in the lower stratosphere, into sulfate aerosol may ultimately affect the earth's radiative balance.[4−6] The conventional procedure of balancing global budgets to ascertain the sources, sinks, and trajectories of atmospheric gases is generally fraught with considerable uncertainties. Thus, for example, the most recent estimates[7,8] indicate that the global sources (1.31 ± 0.25 Tg yr^{-1}) and sinks (1.66 ± 0.79 Tg yr^{-1}) of carbonyl sulfide are balanced to within 0.35 ± 0.83 Tg yr^{-1}. The fact that this margin is significantly larger than the estimated input (0.26 Tg yr^{-1}) required to maintain background aerosol levels[7,9−11] precludes establishing whether OCS is indeed a major precursor of stratospheric sulfate.

The isotopic analysis of atmospheric gases provides an alternative, incisive tool to trace their geochemical cycles.[12] [Note: Sulfur isotopic composition, that is, the ratio $R_{sample} = {}^{34}S/{}^{32}S$, is usually reported relative to an international standard in δ ‰ units:[13] $\delta\ {}^{34}S = 1000 \times (R_{sample}/R_{standard} - 1)$.] Numerous studies have utilized sulfur isotopes to discriminate between anthropogenic and biogenic sources of atmospheric SO_2 and OCS.[3,14−22] The evolution of sulfur isotope ratios in stratospheric aerosol following volcanic eruptions may be particularly informative regarding atmospheric dynamics and background aerosol lifetimes.[23−26]

The OH-radical drives the oxidation of most species in the troposphere and the lower stratosphere, where direct molecular photoexcitation is usually hampered under the ozone layer.[27−30] The gas-phase oxidation of sulfur dioxide into sulfuric acid is considered to proceed via the following reactions:[18,31−37]

$$SO_2 + OH + M \rightleftharpoons HOSO_2 + M \qquad (1, -1)$$

$$HOSO_2 + O_2 \rightarrow HO_2 + SO_3 \qquad (2)$$

in which reaction 1 is rate-limiting under most conditions.[38] Reaction 1 is followed by SO_3 hydration via reaction 3:

$$SO_3 + 2H_2O \rightarrow H_2SO_4 \bullet H_2O \qquad (3)$$

or by SO_3 incorporation into existing aerosol. Elementary considerations suggest that the addition of OH-radicals to SO_2 should display an inverse kinetic sulfur isotope effect,[39] that is, the heavier $^{34}SO_2$ isotopomer should react faster in reaction 1. Recent studies on the contributions of sea-salt sulfate and continental sulfur dioxide to remote marine aerosols and Antarctic ice core sulfate[15,16] implicitly discounted any possible variation of the isotopic composition of SO_2 along its trajectory.[20−22] In fact, the isotopic composition of sulfate aerosol formed by oxidation of SO_2 released from remote sources will ultimately depend on the relative importance of reaction 1 vs heterogeneous oxidation by H_2O_2:[18,40,41]

$$SO_2 + H_2O \rightarrow H^+ + HSO_3^- \qquad (4)$$

$$HSO_3^- + H_2O_2 \rightarrow SO_4^{2-} + H^+ + H_2O \qquad (5)$$

It is apparent that the diagnostic value of isotopes in environmental science cannot be fully realized unless their effects upon the physical and chemical transformations involved are properly quantified. In this paper, we evaluate kinetic sulfur isotope effects for reaction 1 under atmospheric conditions using

* To whom correspondence should be addressed.

10.1021/jp011014+ CCC: $20.00
Published on Web 08/02/2001

TABLE 1: Molecular Parameters Used in the Calculations

species	parameters
OH	$\Delta H_{f,298K} = 39.46$ kJ mol^{-1}; $S°_{298K}$ (standard state: 1 atm ideal gas) = 183.81 J K^{-1} mol^{-1} [a]
$^{32}SO_2$	$\Delta H_{f,298K} = -296.86$ kJ mol^{-1}; $S°_{298K} = 248.37$ J K^{-1} mol^{-1};[a] $I^{1/3} = 28.66$ amu Å^2; $\overline{\nu i}$'s/cm^{-1} = 518, 1151, 1362[b]
$^{34}SO_2$	$I^{1/3} = 28.99$ amu Å^2; $\overline{\nu i}$'s/cm^{-1} = 513, 1145, 1345[b]
$HO^{32}SO_2$	$\Delta H_{f,298K} = -389$ kJ mol^{-1}; $S°_{298K} = 290.8$ J K^{-1} mol^{-1};[a] I$^{1/3} = 71.14$ amu Å^2; $\overline{\nu i}$'s/cm^{-1} = 3540, 1309, 1296, 1097, 759, 252, 500, 400 (2)[c]
$HO^{34}SO_2$	$I^{1/3} = 71.26$ amu Å^2; $\overline{\nu i}$'s/cm^{-1} = 3540, 1293, 1289, 1090, 752, 252, 497, 397 (2)[b]
$[HO\cdots{}^{32}SO_2]^{\ddagger}$	$I^{1/3} = 87.64$ amu Å^2; $\overline{\nu i}$'s/cm^{-1} = 3638, 1100, 900, 300, 200, 100 (2), 80
$[HO\cdots{}^{34}SO_2]^{\ddagger}$	$I^{1/3} = 87.82$ amu Å^2; $\overline{\nu i}$'s/cm^{-1} = 3638, 1090, 892, 297, 198, 99 (2), 80

[a] Reference 33. [b] Reference 46. [c] Reference 49.

unimolecular reaction theory in conjunction with the most reliable ancillary information.

Kinetic Sulfur Isotope Effects in Reaction 1

The fractionation ratio f in reaction 1 is evaluated from the sulfur kinetic isotope effects on the unimolecular decomposition of the hydroxysulfonyl radical $HOSO_2$, $^{34}k_{-1}/^{32}k_{-1}$, which we estimate by means of RRKM theory,[42,43] and the ratio of overall equilibrium constants $^{34}K_1/^{32}K_1$:[39,44]

$$f = \frac{^{34}k_1}{^{32}k_1} = \frac{^{34}k_{-1}}{^{32}k_{-1}}\left[\frac{^{34}K_1}{^{32}K_1}\right] \tag{6}$$

$^{34}K_1/^{32}K_1$ can be obtained from the corresponding ratio of molecular partition functions:[45]

$$\frac{^{34}K_1}{^{32}K_1} = \left[\frac{M_{HO^{34}SO_2}M_{^{32}SO_2}I^{1/3}_{HO^{34}SO_2}I^{1/3}_{^{32}SO_2}}{M_{HO^{32}SO_2}M_{^{34}SO_2}I^{1/3}_{HO^{32}SO_2}I^{1/3}_{^{34}SO_2}}\right]^{3/2}\left[\frac{Q_{HO^{34}SO_2}Q_{^{32}SO_2}}{Q_{HO^{32}SO_2}Q_{^{34}SO_2}}\right] \tag{7}$$

In eq 7, M is the molecular mass, $I = (I_a I_b I_c)$ and is the product of the principal moments of inertia ($I^{1/3}$ in amu Å^2), and Q is the harmonic vibrational partition function:

$$Q = \prod_{i=1}^{3N-6}\frac{\exp(1.444\text{-}\overline{\nu_i}/2T)}{1 - \exp(-1.444\overline{\nu_i}/T)} \tag{8}$$

where the $\overline{\nu_i}$'s are vibrational mode energies in cm^{-1}.

Most of the required molecular data are available or could be estimated by standard procedures. The molecular geometry and vibrational frequencies of the SO_2 isotopomers are well established.[46] We adopted the structures of the $HOSO_2$ (^{2}A) radical[35] and the corresponding transition state $[HO\text{---}SO_2]^{\ddagger}$ recently calculated at the MP2 level.[32] However, we consider that the energy of the transition state is better defined by the experimental high-pressure activation energy of reaction 1, $E_1 = (3.0 \pm 0.8)$ kJ mol^{-1},[33] than by ab initio calculations. Eclecticism is entirely justified in this case, given the unreliability of ab initio calculations in circumscribing the energies of low-barrier transition states. The position of the transition state actually corresponds to a tight configuration, as expected for the addition of a free radical to a closed-shell species.[47] The fact that the HO−SO_2 bond length in the transition state $R_{S-OH} = 2.13$ Å is only 29% longer than the equilibrium value implies that the torsional mode of the OH group remains fully hindered, and may be treated as a vibration, throughout.[48]

Five of the nine internal vibrations of $HOSO_2$ sulfur isotopomers were directly observed by Kuo et al.[49] The remaining four, which include the torsion of the −OH group, a O═S═O bend, and two O−S═O rocks, were assigned on the basis of Nagase et al. calculations.[50] The frequencies of the three SO_3 deformation modes in $HO^{34}SO_2$, that is, those expected to be sensitive to isotopic substitution, were constrained by the Teller−Redlich product theorem:[39,42]

$$\prod_{i}^{3N-6}\frac{\overline{\nu}_{i,\,HO^{34}SO_2}}{\overline{\nu}_{i,\,HO^{34}SO_2}} = \left(\frac{M_{HO^{34}SO_2}I^{1/3}_{HO^{34}SO_2}}{M_{HO^{32}SO_2}I^{1/3}_{HO^{32}SO_2}}\right)^{3/2}\prod_{j}^{N}\left(\frac{m_{j,\,HO^{32}SO_2}}{m_{j,\,HO^{34}SO_2}}\right)^{3/2} \tag{9}$$

All the required parameters used in the calculations are collated in Table 1.

Numerical application of RRKM theory to reaction −1 further requires specifying the vibrational spectrum of the transition state, the energy barrier $E_{-1}°$ at 0 K, plus the Lennard-Jones diameter ($\sigma = 4.1$ Å) and well depth ($\epsilon = 115$ cm^{-1}) values for reactant-bath gas (M = N_2) collisions.[48] We assumed that the three-external rotations of $HOSO_2$ are adiabatic, as expected for a tight transition state, that is, angular momentum is only conserved in the high-pressure limit. The vibrational frequencies of the TS are constrained by its entropy, $S^{\ddagger}°$, which can be obtained from the overall entropy change:

$$\Delta S°_{-1} = S°_{SO_2} + S°_{OH} - S°_{HOSO_2} \tag{10}$$

$\Delta S_{-1}° = 248.37 + 183.81 - 290.80 = 141.38$ J K^{-1} mol^{-1} (standard state: 1 atm = 760 Torr = 1.011×10^5 Pa ideal gas at 300 K), and the experimental value of the high-pressure A-factor for reaction 1:[33,45] $A_{1p,\infty} = A_{1c,\infty}/(eR'T) = (1.2 \times 10^{-11}$ cm^3 molecule^{-1} s^{-1})$(6 \times 10^{20})/(2.7172 \times 0.082$ L atm K^{-1} mol^{-1} $\times$ 300 K) = 1.08×10^8 atm^{-1} s^{-1}, via detailed balance:[45]

$$A_{-1,\infty} = A_{1p,\,\infty}\exp(\Delta S°_{-1}/k_B) = 10^{15.43}\text{ s}^{-1} = (ek_BT/h)\exp[(S^{\ddagger}° - S°_{HOSO_2})/k_B] \tag{11}$$

The vibrational frequencies of $[HO\cdots{}^{32}SO_2]^{\ddagger}$ (Table 1), which are lower than in the $HOSO_2$ radical with the exception of the OH stretching frequency, were adjusted to meet this condition. The critical energy for the dissociation of $HO^{32}SO_2$, reaction (−1), is given by: $^{32}E_{-1}° = \Delta H_{-1,300K}° + \int_{300K}^{0K}\Delta C_{-1,p}° dT + E_1° = (131.6 - 8.1 + 3.0) = 126.50$ kJ mol^{-1}. The corresponding value for $HO^{34}SO_2$ dissociation follows from: $^{34}E_{-1}° = {}^{32}E_{-1}° + \text{ZPE}([HO\cdots{}^{34}SO_2]^{\ddagger}) - \text{ZPE}(HO^{34}SO_2) - \text{ZPE}([HO\cdots{}^{32}SO_2]^{\ddagger}) + \text{ZPE}(HO^{32}SO_2) = 126.62$ kJ mol^{-1}. RRKM calculations were carried out with the UNIMOL program package, using the harmonic oscillator approximation for all vibrational modes. Master equation treatment of weak collisions in the falloff region was dealt with by means of an exponential energy transfer distribution function, using an initial energy grain size of 200 cm^{-1}. The assumed Lennard-Jones

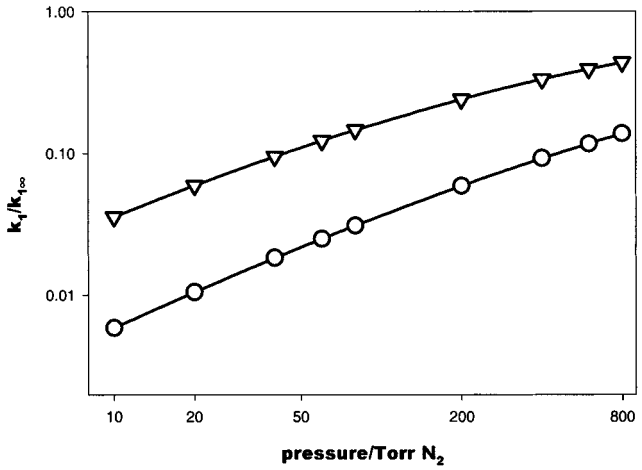

Figure 1. Falloff curves $k_{-1}/k_{-1,\infty}$ for the unimolecular decomposition of $HO^{32}SO_2$ in N_2. ▽: 200 K. ○: 300 K.

parameters lead to an average downward energy transfer per collision of $\langle \Delta E_{down} \rangle = 200$ cm^{-1}, weakly dependent on temperature, which is consistent with an experimental average collisional efficiency $\beta_c \sim 0.2$ for N_2 as bath gas.[33,34]

The results of the calculations are shown in Figures 1 and 2. Our calculated value of $^{32}k_1 \sim 1 \times 10^{-13}$ cm^3 molecule^{-1} s^{-1} at [M] $= 1 \times 10^{18}$ molecules cm^{-3}, 300 K, is within a factor of 2 of the experimental value, as measured by Wine et al.,[34] and Fulle et al.[33] in N_2 as a bath gas. Further refinements are not warranted at this time (see below). More importantly, we find that sulfur isotopes indeed induce an inverse primary kinetic isotope effect, that is, $^{34}SO_2$ reacts faster than $^{32}SO_2$ in reaction 1. The unimolecular dissociation of the $HOSO_2$ radical, reaction −1, behaves similarly. The reason for the latter is that the denser vibrational manifolds of both $HO^{34}SO_2$ and $[HO\cdots{}^{34}SO_2]^{\ddagger}$ overcome the small, but positive difference of critical energies $^{34}E_{-1}^{\circ} - {}^{32}E_{-1}^{\circ} > 0$, that would otherwise cause a *direct* isotope effect, under all conditions. This outcome has a purely statistical origin and is unrelated to conventional secondary isotope effects. Actually, the ratio of the high-pressure *A*-factors: $^{34}A_{-1,\infty}/{}^{32}A_{-1,\infty} = 1.096$, is very similar to the ratio of the low-pressure rate coefficients $^{34}k_{-1,0}/{}^{32}k_{-1,0} = 1.070$, and accounts for a substantial fraction of the calculated effect. The ratio of equilibrium constants [$(^{34}K_1/{}^{32}K_1) = 1.048$ and 1.031 at 200 and 300 K, respectively] further adds to the trend (see eq 6). The pressure and temperature dependences of the fractionation ratio *f* within the ranges covered in Figure 3 (P/Torr ≤ 760 and 200 ≤ T/K ≤ 300) is given by eq 12:

$$f = 1.1646 + 0.0198P^{0.1769} - 0.3092(T/1000) \quad (12)$$

The parameters in eq 12 are mostly sensitive to the input $A_{1,\infty}$ value in eq 11, which, in conjunction with the estimated entropy of $HOSO_2$, determines $A_{-1,\infty}$ and, hence, the properties of the transition state. As mentioned before, we adopted the most recent $A_{1,\infty} = 1.2 \times 10^{-11}$ molecule cm^{-3} s^{-1}, $E_1 = 3.0$ kJ mol^{-1} values derived by extrapolation of experimental rates determined up to 96 bar,[33] instead of the lower values measured by Wine et al. below 1 bar.[34] However, we observe that the derived $^{32}A_{1,\infty} = 10^{15.43}$ s^{-1} value (300 K) is consistent with a relatively loose transition state despite of the fact that reaction 1 involves the addition of OH-radicals to a closed-shell species.[45,47] A lower $^{32}A_{1,\infty}$ value will result from a larger $S^{\circ}_{HOSO_2}$ value but, again, we find no plausible arguments for making any such corrections, particularly vis-à-vis reliable,

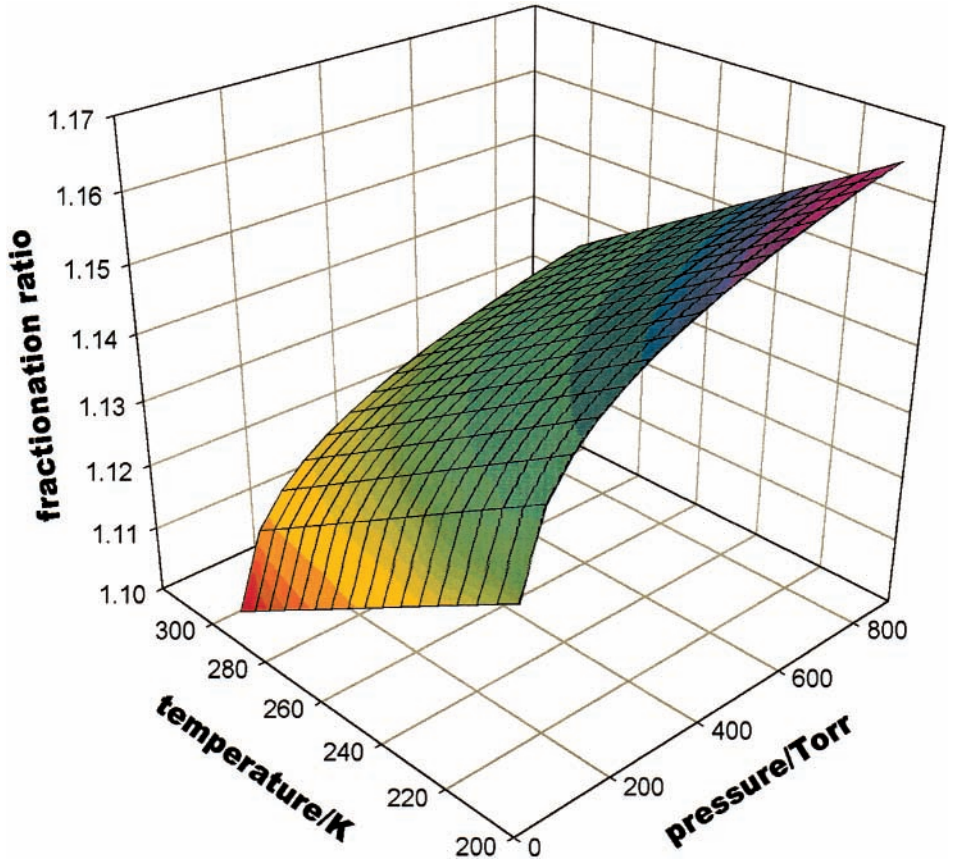

Figure 2. Fractionation ratios $f = (k_{OH+^{34}SO_2})/(k_{OH+^{32}SO_2})$ as function of pressure and temperature. The depicted surface corresponds to $f = 1.1646 + 0.0198(P/\text{Torr})^{0.1769} - 0.3092[(T/\text{K})/1000]$.

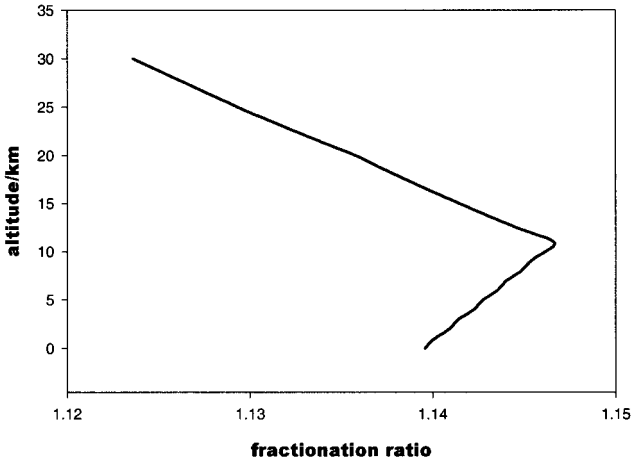

Figure 3. Fractionation ratios $f = f[P(z),T(z)]$ as function of the altitude z. The implicit $P(z)$ and $T(z)$ vertical profiles correspond to the 1976 standard atmosphere.[1]

direct data.[49,50] Furthermore, a loose transition state would require a ratio $\rho = r^{\ddagger}_{S-OH}/r_{S-OH}$ somewhat larger than the $\rho = 1.29$ value based on ab initio calculated geometries.[32,45] Bearing these uncertainties in mind, we performed a numerical sensitivity analysis indicating that a 10-fold reduction in $A_{-1,\infty}$ will lower f by about 0.05 units across the (P,T) ranges investigated. In other words, any adjustments to present parameters could not detract from our conclusion that $f > 1.07$ under atmospheric conditions. Any further improvements would necessarily call for higher-level ab initio calculations of the position and structure of the transition state.[51]

Present results illuminate the early observations of Castleman et al. on the sulfur isotopic signatures of stratospheric sulfate aerosol following the major volcanic eruption of Mt. Agung.[23,24] The aerosol formed initially at 19 km altitude was enriched in ^{34}S, peaking at $\delta^{34}S \sim +20‰$ about 100 days after the eruption, an event that preceded maximum aerosol concentrations by about 200 days. The initial phase was followed by a precipitous decline of ^{34}S-sulfate aerosol abundance down to $\delta^{34}S = -24‰$ levels about 800 days after the eruption, before slowly recovering the background value of $\delta^{34}S = +2.6‰$. From the perspective of present results, this behavior is consistent with the OH-driven oxidation of a finite stratospheric SO_2 load into prompt $^{34}SO_4$-enriched aerosol that undergoes concomitant sedimentation. The ulterior falloff of $\delta^{34}S$ values naturally ensues from the progressive depletion of ^{34}S in the remaining SO_2 pool, a process known as Rayleigh distillation.[15,52] The observed enrichment of tropospheric sulfate aerosol in ^{34}S relative to SO_2, together with the fact that SO_2 oxidation rates increase during the summer months,[53] is also consistent with $f > 1$ for the combined gas-phase oxidation processes, among which reaction 1 is dominant,[30] despite suggestions to the contrary.[18,53]

References and Notes

(1) Seinfeld, J. H.; Pandis, S. N. *Atmospheric Chemistry and Physics: From Air Pollution to Climate Change*; John Wiley and Sons: New York, 1998.

(2) Andreae, M. O.; Crutzen, P. J. *Science* **1997**, *276*, 1052−1058.

(3) Turekian, K. K.; Tanaka, N. *Geophys. Res. Lett.* **1992**, *19*, 1767−1770.

(4) Hamill, P.; Jensen, E. J.; Russell, P. B.; Bauman, J. J. *Bull. Am. Meteorol. Soc.* **1997**, *78*, 1395−1410.

(5) Turco, R. P.; Whitten, R. C.; Toon, O. B.; Pollack, J. B.; Hamill, P. *Nature* **1980**, *283*, 283−286.

(6) Brock, C. A.; Hamill, P.; Wilson, J. C.; Jonsson, H. H.; Chan, K. R. *Science* **1995**, *270*, 1650−1653.

(7) Kjellstrom, E. *J. Atmos. Chem.* **1998**, *29*, 151−177.

(8) Watts, S. F. *Atmos. Environ.* **2000**, *34*, 761−779.

(9) Chin, M.; Davis, D. D. *J. Geophys. Res.* **1995**, *100*, 8993−9005.

(10) Grant, W. B.; Browell, E. V.; Long, C. S.; Stowe, L. L.; Grainger, R. G.; Lambert, A. *J. Geophys. Res.* **1996**, *101*, 3937−3988.

(11) Weisenstein, D. K.; Yue, G. K.; Ko, M. K. W.; Sze, N.-D.; Rodriguez, J. M.; Scott, C. J. *J. Geophys. Res.* **1997**, *102*, 13019−13035.

(12) Wahlen, M. In *Stable Isotopes in Ecology and Environmental Science*; Lajtha, K., Michener, R. H., Eds.; Blackwell: Cambridge, MA, 1994; pp 93−113.

(13) Beaudoin, G.; Taylor, B. E.; Rumble, D., III; Thiemens, M. *Geochim. Cosmochim. Acta* **1994**, *58*, 4253−5255.

(14) McArdle, N. C.; Liss, P. S. *Atmos. Environ.* **1995**, *29*, 2553−2556.

(15) Newman, L.; Krouse, H. R.; Grinenko, V. A. In *Sulphur isotope variations in the atmosphere*; Krouse, H. R., Grinenko, V. A., Eds.; Wiley: New York, 1991.

(16) Nielsen, H. *Tellus* **1974**, *26*, 213−221.

(17) Panettiere, P.; Cortecci, G.; Dinelli, E.; Bencini, A.; Guidi, M. *Appl. Geochem.* **2000**, *15*, 1455−1467.

(18) Tanaka, N.; Rye, D. M.; Xiao, Y.; Lasaga, A. C. *Geophys. Res. Lett.* **1994**, *21*, 1519.

(19) Tanaka, N.; Turekian, K. K. *Nature* **1991**, *352*, 226−228.

(20) Patris, N.; Delmas, R. J.; Jouzel, J. *J. Geophys. Res.* **2000**, *105*, 7071−7078.

(21) Patris, N.; Mihalopoulos, N.; Baboukas, E. D.; Jouzel, J. *J. Geophys. Res.* **2000**, *105*, 14449−14457.

(22) Norman, A. L.; Barrie, L. A.; Toom-Sauntry, D.; Sirois, A.; Krouse, H. R.; Li, S. M.; Sharma, S. *J. Geophys. Res.* **1999**, *104*, 11619−11631.

(23) Castleman, J. A. W.; Munkelwitz, H. R.; Manowitz, B. *Tellus* **1974**, *26*, 222−234.

(24) Castleman, J. A. W.; Munkelwitz, H. R.; Manowitz, B. *Nature* **1973**, *244*, 345−346.

(25) Forrest, J.; Newman, L. *Atmos. Environ.* **1973**, *7*, 561−573.

(26) Bekki, S. *Geophys. Res. Lett.* **1995**, *22*, 913−916.

(27) Hanisco, T. F.; Lanzendorf, E. J.; Wennberg, P. O.; Perkins, K. K.; Stimpfle, R. M.; Voss, P. B.; Anderson, J. G.; Cohen, R. C.; Fahey, D. W.; Gao, R. S.; Hintsa, E. J.; Salawitch, R. J.; Margitan, J. J.; McElroy, C. T.; Midwinter, C. *J. Phys. Chem. A* **2001**, *105*, in press.

(28) Tyndall, G. S.; Ravishankara, A. R. *Int. J. Chem. Kinet.* **1991**, *23*, 483−527.

(29) Warneck, P. *Phys. Chem. Chem. Phys.* **1999**, *1*, 5471−5483.

(30) Eggleton, A. E. J.; Cox, R. A. *Atmos. Environ.* **1978**, *12*, 227.

(31) Jayne, J.; Poschl, U.; Chen, Y.; Dai, D.; Molina, L.; Worsnop, D.; Kolb, C.; Molina, M. *J. Phys. Chem. A* **1997**, *101*, 10000.

(32) Li, W.-K.; McKee, M. L. *J. Phys. Chem. A* **1997**, *101*, 9778−9782.

(33) Fulle, D.; Hamann, H. F.; Hippler, H. *Phys. Chem. Chem. Phys.* **1999**, *1*, 2695−2702.

(34) Wine, P. H.; Thompson, R. J.; Ravishankara, A. R.; Semmes, D. H.; Gump, T. A.; Nicovich, J. M. *J. Phys. Chem.* **1984**, *88*, 3314.

(35) Majumdar, D.; Kim, G.-S.; Kim, J.; Oh, K. S.; Lee, J. Y. *J. Chem. Phys.* **2000**, *112*, 723−730.

(36) Kolb, C. E.; Jayne, J. T.; Worsnop, D. R.; Molina, M. J.; Meads, R. F.; Viggiano, A. A. *J. Am. Chem. Soc.* **1994**, *116*, 10314.

(37) Morokuma, K.; Muguruma, C. *J. Am. Chem. Soc.* **1994**, *116*, 10316.

(38) Gleason, J. F.; Sinha, A.; Howard, C. J. *J. Phys. Chem.* **1987**, *91*, 9.

(39) van Hook, W. A. In *Isotope effects in chemical reactions*; ACS Monograph 167; Collins, C. J., Bowman, N. S., Eds.; American Chemical Society: New York, 1970; Vol. 167, pp 1−84.

(40) Eriksen, T. D. *Acta Chem. Scand.* **1972**, *26*, 573−580.

(41) Hegg, D.; Hobbs, P. *Atmos. Environ.* **1978**, *12*, 241.

(42) Robinson, P. J.; Holbrook, K. A. *Unimolecular reactions*; Wiley: London, 1972; Chapter 9.

(43) Forst, W. *Theory of unimolecular reactions*; Academic Press: New York, 1973.

(44) Weston, J. R. E. *J. Phys. Chem. A* **2001**, *105*, 1656.

(45) Benson, S. W. *Thermochemical Kinetics*, 2nd ed.; Wiley-Interscience: New York, 1976.

(46) Allavena, M.; Rysnik, R.; White, D. *J. Chem. Phys.* **1969**, *50*, 3399-.

(47) Grela, M. A.; Colussi, A. J. *Int. J. Chem. Kinet.* **1987**, *19*, 869−879.

(48) Gilbert, R. G.; Smith, S. C. *Theory of Unimolecular and Recombination Reactions*; Blackwell Scientific Publications: Oxford (UK), 1990.

(49) Kuo, Y.-P.; Cheng, B.-M.; Lee, Y.-P. *Chem. Phys. Lett.* **1991**, *177*, 195−199.

(50) Nagase, S.; Hashimoto, S.; Akimoto, H. *J. Phys. Chem.* **1988**, *92*, 641.

(51) Colussi, A. J.; Blanco, M.; Leung, F. Y.; Hoffmann, M. R., to be submitted.

(52) Griffith, D. W. T.; Toon, G. C.; Sen, B.; Blavier, J. F.; Toth, R. A. *Geophys. Res. Lett.* **2000**, *27*, 2485−2488.

(53) Saltzman, E. S.; Brass, G. W.; Price, D. A. *Geophys. Res. Lett.* **1983**, *10*, 513.